An Open Platform for Simulating the Physical Layer of 6G Communication Systems with Multiple Intelligent Surfaces

Alexandros Papadopoulos
CSE Dept. & Information Technologies Institute
University of Ioannina & CERTH
Ioannina, Greece
a.papadopoulos@uoi.gr

Antonios Lalas
Information Technologies Institute
CERTH
Thessaloniki, Greece
lalas@iti.gr

Konstantinos Votis
Information Technologies Institute
CERTH
Thessaloniki, Greece
kvotis@iti.gr

Dimitrios Tyrovolas
ECE Dept.
Aristotle University of Thessaloniki
Thessaloniki, Greece
tyrovolas@auth.gr

George Karagiannidis
ECE Dept.
Aristotle University of Thessaloniki
Thessaloniki, Greece
geokarag@auth.gr

Sotiris Ioannidis
ECE Dept.
TUC & FORTH
Chania, Greece
sotiris@ece.tuc.gr

Christos Liaskos
CSE Dept.
University of Ioannina & FORTH
Ioannina, Greece
cliaskos@uoi.gr

***Abstract*—Reconfigurable Intelligent Surfaces (RIS) constitute a promising technology that could fulfill the extreme performance and capacity needs of the upcoming 6G wireless networks, by offering software-defined control over wireless propagation phenomena. Despite the existence of many theoretical models describing various aspects of RIS from the signal processing perspective (e.g., channel fading models), there is no open platform to simulate and study their actual physical-layer behavior, especially in the multi-RIS case. In this paper, we develop an open simulation platform, aimed at modeling the physical-layer electromagnetic coupling and propagation between RIS pairs. We present the platform by initially designing a basic unit cell, and then proceeding to progressively model and simulate multiple and larger RISs. The platform can be used for producing verifiable stochastic models for wireless communication in multi-RIS deployments, such as vehicle-to-everything (V2X) communications in autonomous vehicles and cybersecurity schemes, while its code is freely available to the public.**

***Index Terms*—Wireless, communication, propagation, software-defined, 6G, verifiable channel models, networks, metamaterials, metasurfaces, RIS.**

I. Introduction

The coming of 6G wireless communications renders as priority the realization of the, until now, uncontrollable communication environment as a programmable resource [1]. The utilization of the metasurfaces–recently popularized in the communications society under the term Reconfigurable Intelligent Surfaces (RISs) [2]–could play a game changer role in the manipulation of the communication field. The key indicator is that, instead of considering environmental reflection and scattering as uncontrollable phenomena whose impacts can only be described stochastically, they could be considered as parameters of the network that should be optimized [3].

RISs mainly are planar and rectangular, tile-resembling devices whose physical characteristics, and particularly their permittivity and permeability, can be engineered in real-time to obtain a required macroscopic electromagnetic behavior [3]. Thus, when a wireless wave emitted by a user device (e.g., a smartphone) impinges upon an RIS, it can be programmatically reflected to any custom direction, or even be split among several ones. Based on this property, a popular demo case of the RISes is the establishment of *effective LOS (line of sight) conditions* between a transmitter and a receiver who are actually in NLOS [3]. Furthermore RIS uses include the mitigation of multi-path fading phenomena, the overcoming of localized coverage holes and the optimal energy management in IoT systems [3], [4]. Moreover, RISs could assist in the design of low-complexity and energy-efficient massive Multiple-Input-Multiple-Output (MIMO) transmitting and receiving antennas, meeting a very promising expectation of 5G and Beyond-5G (B5G) networks [5]. Since RISes can act as generic facilitators of the communication links between base stations and the end-users, their system use cases are abundant. Smart homes, cities, hospitals and industries are theorized to benefit greatly via the RIS technology. Moreover, the utilization of RISes in vehicle-to-everything (V2X) communications could overcome the current challenges stemming from the acute fading and Doppler shift suffered is these systems [6], [7].

Due to their significant potential, several RIS-enabled channel models have been proposed. Indicatively: in [8], multiple RIS are employed to support Non-Orthogonal-Multiple-Access (NOMA) networks; in [9], the closed-form expressions for the behavior of cascaded multi-RISs are presented; in [10], the performance of a single RIS for time-division multiple access (TDMA), frequency-division multiple access (FDMA), and NOMA is presented. However, despite multiple channel models proposed, simulating the physics of such a system remains a task for the physicist, and not usable by wireless

978-3-903176-51-5 © 2022 IFIP

engineers in general.

The contribution of this paper is a physics simulation platform for studying the communication between any RIS couple of a multi-RIS deployment. The platform is open and freely available [11], and provides the tool for exploring the wireless propagation environment between RIS units in any ecosystem. This can be used for deducing accurate wireless channel models, validated via actual physics simulations, enabling a variety of application domains, such as V2X communications, especially in autonomous vehicles (AVs), as well as cybersecurity defence mechanisms.

The remainder of this paper is organized as follows. In Section II we present the RIS system model employed by the platform. In Section III we present the design methodology of the proposed platform. Section IV demonstrates use cases built with the platform, and the paper is concluded in Section V.

II. System Model and Related Studies

The proposed platform models the accurate electromagnetic propagation between two RIS units–whose composition, dimensions, and state are user-defined–while varying the distance between them. Each RIS consists of a planar arrangement of elements, known as cells in the metasurface terminology [12]. In the following, we employ the Square Split Ring Resonators [13] (S-SRR) design for each RIS cell as a running example and for ease of elucidation. Each element hosts a port and a lumped element offering tunable impedance within a user-specified range. We consider that all the elements of the RIS_1 are active, meaning that power is generated at each of their ports, enters the system and is altered by the state of the corresponding lumped element. Additionally, all the elements of the RIS_2 are passive, meaning that their ports receive power emanated from RIS_1, alter it based on the state of the local lumped element and re-emit it. Depending on its configuration, this setup emulates either: i) the RIS-RIS part of a transmitter-RIS-RIS-receiver communication, which is useful for deriving verifiable stochastic models for the inter-RIS part of a channel. ii) the transmitter-RIS or the RIS-receiver part of the communication. (E.g., in order to study the transmitter-RIS part, one simply sets the number of elements of RIS_1 to 1).

Accounting for the capability to freely vary the distance between the two RIS units (center-to-center), the proposed platform becomes a versatile tool for uniformly studying any part of a multi-RIS system. In any customization, the platform treats the element lumped states as optimization parameters and seeks to maximize the power transfer from RIS_1 to RIS_2 for the given physical RIS composition and distance. The outputs of the simulation are the s-parameters from every port of RIS_1 to every port of RIS_2. The user can then define any post-processing of the produced s-parameters, e.g., for producing an inter-RIS path-loss model versus their distance. At the core of the platform, we utilize the open-source Finite-difference time-domain (FDTD) solver OpenEMS [14].

In our past work, we developed an experimental testbed for evaluating networked RIS units, without, however, including a multi-RIS simulation platform [15]. On the other hand, there is an extensive body work dedicated to the stochastic modeling of RIS-enabled channels that would benefit from such a tool. Indicatively, in [16], the programming of the reflection coefficients of the unit cells is examined for the optimal performance of the metasurfaces. In [17], indoor and outdoor scenarios are examined in various frequency bands. In [10], the performance of a single RIS for time-division multiple access (TDMA), frequency-division multiple access (FDMA), and NOMA is presented. In [6], theoretical models for the optimization and resource allocation in V2X networks are examined. Lastly, SimRIS Channel Simulator is presented in [18]. This tool generates the matrices of channels coefficients among the transmitter, a single RIS and receiver assuming theoretical channel models as its basis (e.g., between elements), and without actually simulating the underlying physics. To the best of our knowledge, there is no structured and open platform for studying the physical layer of RIS communication. We make the source code of our platform freely available in Github [11].

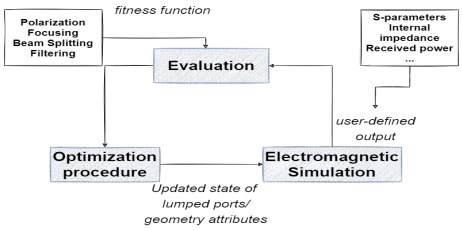

Fig. 1. Computational workflow of optimization procedure.

III. Platform Design and Methodology

A. RIS pair optimization Method

The general optimization workflow is depicted in Figure 1. The goal of the optimization procedure is the detection of the optimal configuration of the RIS unit. As configuration, the state of the unit cell's lumped ports or the geometry attributes of the RISs could be considered. The candidate configuration is inserted to the electromagnetic simulation module. In this component, the physical layer of the RIS units is modelled. The user-defined outputs, e.g., s-parameters, internal impedance, received power etc, are utilized for the evaluation of the system's performance. In the evaluation component, the simulator's output is compared with a given fitness function that describes the desired functionality of the RIS elements. The RIS unit is able to support multiple functionalities such as the change of the reflected wave polarization, the focusing of the reflected waves to a specific direction, the beam splitting in more targets or the filtering of a specific frequency band.

The result of the evaluation processing is directed again in the Optimization Procedure module in order the new candidate configuration to be generated. In this step, any optimization method, e.g., a Genetic Algorithm, a Differential Evolution or a Particle Swarm Optimization, could be utilized. The procedure ends once the level of fitness is deemed as satisfactory or the maximum available amount of time is devoted.

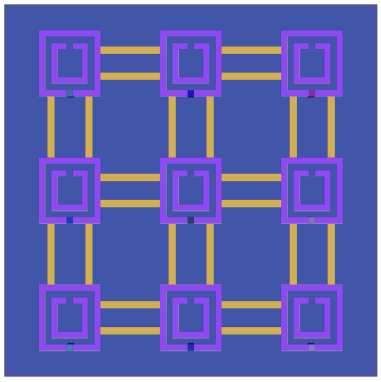

Fig. 2. 3x3 RIS with load patches.

B. Electromagnetic Simulation

The electromagnetic simulation could be established in the proposed simulation platform that consists of two main parts; the *unit cell definition* and the *RIS pairs simulation*. Initially, *unit cell definition* is utilized for the design of the unit cell. The unit cell consists of the substrate, the groundplane and the S-SRR. The properties of the substrate are user-defined while the groundplane and the S-SRR are layers of metal. In the gap of S-SRR's outer ring, a lumped port is positioned. This port could radiate or not. The radiation is a Gaussian excitation.

In the next step, the *RIS pairs simulation* creates two identical metasurfaces composed by periodically positioned, identical, unit cells. The S-SRRs are connected with the adjacent ones via load patches (Figure 2). The distance between the RIS pairs is, also, user-defined.

The s-parameters is the basic output of the simulator, which can then be post-processed into any fitness function of interest, to guide the optimization as required by the user. Generally, the s-parameters in a network express the transfer of power from an active port (source) to another that could be passive or not (reference). When the port that acts as source is identical with the reference, the corresponding parameter is called reflection coefficient. In the case that the source and the reference is considered in different ports, the respective parameter is called transmission coefficient. The transmission coefficient is a measurement about the energy coupling between an active and a passive port. The simulation calculates the following:

- The feed point impedance of the active ports.
- The incoming, reflected and accepted (subtraction of incoming and reflected) power in both active and passive ports.
- The reflection coefficients of the active ports and the transmission coefficients of them with the passive ones (s-parameters).
- The resonating frequency in which the reflection coefficients of the active ports are minimized.
- The values of frequency in which the active ports exhibit the maximized transmission coefficients with the passive ones.

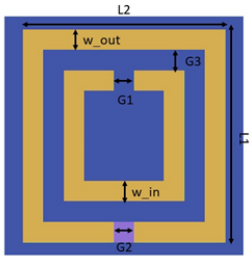

Fig. 3. Unit cell's substrate (blue) and S-SRR (yellow).

C. Unit cell definition

The first step is the design of the RISs' unit cell. In the *unit cell definition*, the user is able to re-adjust:

- The central frequency and the bandwidth of the Gaussian excitation.
- The dimensions of S-SRRs (Figure 3).
- The properties (electric permittivity, ϵ_r, and tangent loss, *tand*) and the dimensions of substrate (width, length and thickness).
- The distance between the pair of unit cells. By default, the distance is 10 mm.

The resonating frequency displays strong dependency with the length, the width and the distance of the S-SRRs' rings. The widths of the rings' patch and the gaps do not impact significantly on the behavior of S-SRRs' resonating frequency. As concerns the substrate, its dimensions affect directly and strongly both the resonating frequency and the coupling between the active and the passive ports. Hence, we propose the dedicated variables to be utilized wisely.

The fine tuning evaluation is based on s-parameters and the feed point impedance. Having defined the port of the first unit cell active and the other one's passive, we expect to observe minimization of the reflection coefficient and maximization of the transmission one at the central frequency. As concerns the feed point impedance, the internal resistance of ports has been set to 50 Ω. Therefore, the real and imaginary part of feed point impedance should be as close as possible to 50 Ω and 0Ω, correspondingly, in order the maximum power transfer in the central frequency to be achieved.

D. RIS pairs simulation

The first action in the *RIS pairs simulation* is the definition of the S-SRRs dimensions as they have resulted from the *unit cell definition* procedure. Thus, the user is able to re-adjust:

- The dimension of the RIS pairs. The dimension displays the number of the unit cells per row and column.
- The distance between the RIS units.
- The distance between the S-SRRs.
- The width and the thickness of the load patches.

The aforementioned parameters can configure the resonating frequency of the active ports and the coupling of them with the passive ones.

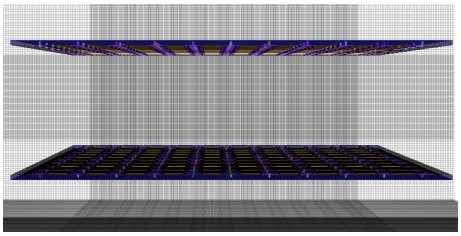

Fig. 4. The format of the 11x11 RIS pairs.

E. Meshing in OpenEMS

In the FDTD solvers, a main task is the design of the optimal meshing. The meshing is a strictly rectilinear structure that separates the observed area into many, small cells. Its optimal design ensures the minimization of the running time and the maximization of the measurements accuracy. We have adapted the meshing structure in order the simulation of a multiple-component structure to be feasible. The main logic is based on the following statements:

- The resolution expresses the size of the minimal meshing cells. We have introduced two resolution values. The maximum resolution is utilized for the finer structures, e.g., the gaps of S-SRRs. In the coarser structures, e.g., in the surrounding air, we use the coarse resolution value.
- We implement a function that intervenes to avoid a long-time simulation in the case that the distance between adjacent meshing lines becomes less than a pre-defined threshold in each axis. By default, this threshold is equal to the half of the maximum resolution.

IV. Evaluation: Use Cases

In this section, we use the simulation platform for the modeling of 11x11 RIS pairs (Figure 4). This setup can exemplary be used for studying two RIS units placed on opposing walls in a floor plan. The central frequency was selected at 8 GHz and the bandwidth at 2 GHz.

Step 1: We utilize the *unit cell definition* in order the fine tuning to be achieved. We use a substrate with ϵ_r=2.2 and tangent loss tand=0.024. After the required tests, for S-SRR to resonate at the frequency of 8 GHz, the length of the outer ring must be L2=10.36 mm and the respective width L1=10.9 mm. The gap of the outer and the inner ring is G1=G2=1.05 mm. The width of the S-SRRs patches is w_{out}=w_{in}=1.05 mm. As concerns the dimension of the substrate, its length is concluded to be equal to its width, at 12.21 mm, and its thickness is 4.8 mm. Observing Figures 5 and 6, the S-SRRs function properly in the central frequency. This indicates that the fine tuning procedure has been completed.

Step 2: Before we proceed to the simulation of the 11x11 RIS pairs, we work on the 3x3 structure in order the fine tuning of the multiple components to be examined in less time and with lower computational resources. We keep the calculated dimensions of the S-SRR stable.

Using the *RIS pair simulation*, we concentrate on the dimensions of load patches and the distance between the

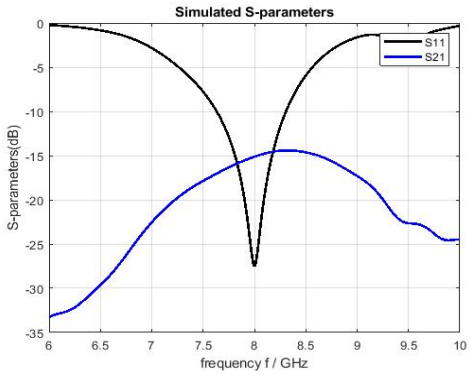

Fig. 5. S-parameters of the S-SRR.

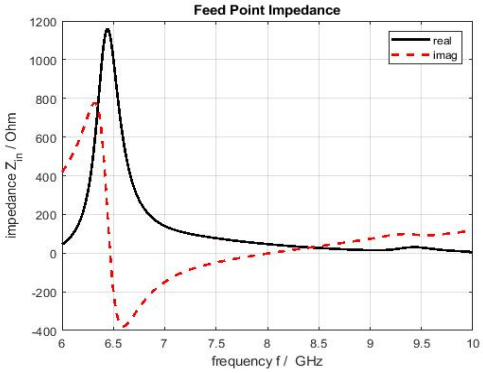

Fig. 6. Feed point impedance of the S-SRR.

adjacent S-SRRs. As it has already been mentioned, these variables have great impact on the resonating frequency and the coupling. After the required tests, the width of the load patches is 1.2 mm, very close to S-SRR's patch width. The distance between the S-SRRs in both horizontal and vertical axis is 10 mm. This value is about equal to the half of the wavelength in the substrate material. An extra option that is available to the user in order to reinforce the coupling is the limitation of the substrate's thickness.

In Figure 7, the blue line represents the reflection coefficient, the red ones depict the transmission parameters among the active elements and the black ones among the passive. It is clear that there is coupling between the active and the passive ports. However, the existence of many active components results in that the resonance is not held in the central frequency for all the unit cells. Despite the fact that there in no common behavior for all the unit cells, it is observed that these ones, which are geometrically symmetric, act similarly (resonating frequency and coupling with the ports).

Step 3: In this phase all the parameters of the system have already been defined. In the *RIS pair simulation*, we just change the dimension of the RIS in order the 11x11 setup to be created. In the Figure 8, the behavior of an active port is depicted. We can point out that the majority of the active ports exhibit resonances in two bands; one with central frequency at 8 GHz with bandwidth about 200 MHz and another one with

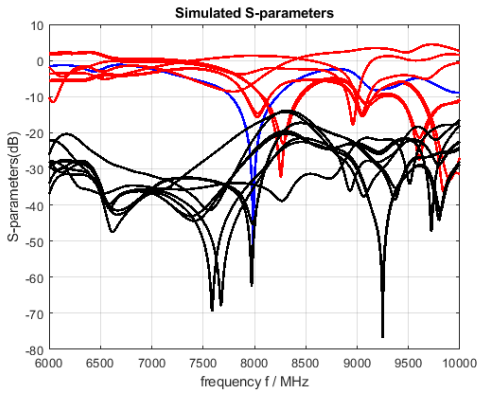

Fig. 7. S-parameters of an active port with patches in 3x3 RIS pairs.

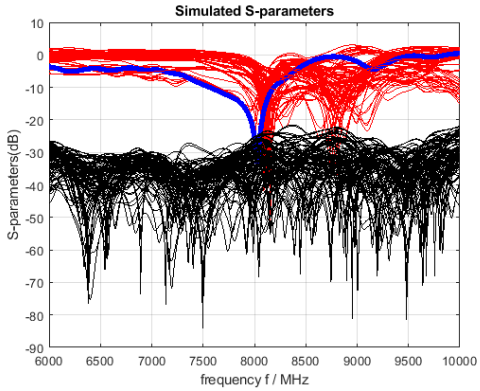

Fig. 8. S-parameters of an active port in 11x11 RIS pairs.

central frequency at 8.9 GHz with bandwidth about 250 MHz.

Once the design is completed, the behavior of the RIS pairs in different distances could be investigated without any update in the structure. The products of this simulation compose a sufficient dataset for the building of custom fitness functions, and the implementation of the optimization procedure accordingly.

V. Conclusion and Future Work

In this paper, a simulation platform for the study of multiple RIS deployments in the physical layer is presented. The proposed platform is able to simulate RIS pairs of any composition and dimensions, and at varying distances between them. The platform provides facilities for pinpointing the resonating frequency of the defined RIS pair, and then for optimizing the energy flow from one to the other. The optimization can be customized for any fitness criterion, and for any tunable state supported by the user-defined RIS designs. The intended use is the exploitation of the produced simulation data for validating theoretical channel models of RIS-empowered system setups. Due to its supported parameterization, the platform can be employed not only for studying the RIS-RIS communication, but also for the MIMO(user)-RIS part of a communication.

Future work is directed towards showcasing the potential of the platform towards creating realistic channel models for indoor and outdoor, RIS enabled environments, such as V2X infrastructure in AVs, enabling also cybersecurity aspects.

VI. Acknowledgment

This work was funded by the projects WISAR (Foundation for Research and Technology–Synergy Grants 2022) for theoretical design, SHared automation Operating models for Worldwide adoption (SHOW) under Grant Agreement No. 875530, for practical design and applicability study on vehicular communications, and COLLABS (EU Horizon 2020, GA 871518) for applicability study on cybersecurity aspects.

References

[1] C. Liaskos *et al.*, "Using any surface to realize a new paradigm for wireless communications," *Commun. ACM*, vol. 61, pp. 30–33, 2018.

[2] M. Di Renzo *et al.*, "Smart radio environments empowered by reconfigurable intelligent surfaces: How it works, state of research, and road ahead," *arXiv preprint arXiv:2004.09352*, 2020.

[3] C. Liaskos *et al.*, "On the network-layer modeling and configuration of programmable wireless environments," *IEEE/ACM Trans. Netw.*, vol. 27, no. 4, pp. 1696–1713, 2019.

[4] E. Basar *et al.*, "Wireless communications through reconfigurable intelligent surfaces," *IEEE access*, vol. 7, pp. 116753–116773, 2019.

[5] H. Wymeersch and B. Denis, "Beyond 5g wireless localization with reconfigurable intelligent surfaces," in *ICC 2020-2020 IEEE International Conference on Communications (ICC)*, pp. 1–6, IEEE, 2020.

[6] X. Gu *et al.*, "Socially aware v2x networks with ris: Joint resource optimization," *IEEE Transactions on Vehicular Technology*, 2022.

[7] Y. U. Ozcan *et al.*, "Reconfigurable intelligent surfaces for the connectivity of autonomous vehicles," *IEEE Transactions on Vehicular Technology*, vol. 70, no. 3, pp. 2508–2513, 2021.

[8] Y. Cheng *et al.*, "Non-orthogonal multiple access (noma) with multiple intelligent reflecting surfaces," *IEEE Transactions on Wireless Communications*, vol. 20, no. 11, pp. 7184–7195, 2021.

[9] D. Tyrovolas *et al.*, "Performance analysis of cascaded reconfigurable intelligent surface networks," *IEEE Wireless Communications Letters*, 2022.

[10] J. Xu and Y. Liu, "A novel physics-based channel model for reconfigurable intelligent surface-assisted multi-user communication systems," *IEEE Transactions on Wireless Communications*, vol. 21, no. 2, pp. 1183–1196, 2021.

[11] A. Papadopoulos, "Github - an open platform for simulating the physical layer of 6g communication systems with multiple intelligent surfaces." https://github.com/alexpapad95/6G-simulation-platform. (Accessed on 09/09/2022).

[12] A. Li *et al.*, "Metasurfaces and their applications," *Nanophotonics*, vol. 7, no. 6, pp. 989–1011, 2018.

[13] C. Milias *et al.*, "Metamaterial-inspired antennas: A review of the state of the art and future design challenges," *IEEE Access*, 2021.

[14] T. Liebig *et al.*, "openems–a free and open source equivalent-circuit (ec) fdtd simulation platform supporting cylindrical coordinates suitable for the analysis of traveling wave mri applications," *International Journal of Numerical Modelling: Electronic Networks, Devices and Fields*, vol. 26, no. 6, pp. 680–696, 2013.

[15] The VISORSURF consortium, *The Internet of Materials*. CRC Press, 2020.

[16] W. Tang *et al.*, "Wireless communications with reconfigurable intelligent surface: Path loss modeling and experimental measurement," *IEEE Transactions on Wireless Communications*, vol. 20, no. 1, pp. 421–439, 2020.

[17] I. Yildirim *et al.*, "Modeling and analysis of reconfigurable intelligent surfaces for indoor and outdoor applications in future wireless networks," *IEEE transactions on communications*, vol. 69, no. 2, pp. 1290–1301, 2020.

[18] E. Basar and I. Yildirim, "Simris channel simulator for reconfigurable intelligent surface-empowered communication systems," in *2020 IEEE Latin-American Conference on Communications (LATINCOM)*, pp. 1–6, IEEE, 2020.